Rigidity dependent knee and cosmic ray induced high energy neutrino fluxes

Journal of Cosmology and Astroparticle Physics
An IOP and SISSA journal

Rigidity dependent knee and cosmic ray induced high energy neutrino fluxes

Julián Candia[1] **and Esteban Roulet**[2]

[1] Departamento de Física, Universidad Nacional de La Plata, CC67, La Plata 1900, Argentina
[2] CONICET, Centro Atómico Bariloche, Av. Bustillo 9500, Bariloche 8400, Argentina
E-mail: candia@venus.fisica.unlp.edu.ar and roulet@cab.cnea.gov.ar

Received 1 July 2003, in final form 13 July 2003
Accepted 25 August 2003
Published 16 September 2003
Online at stacks.iop.org/JCAP/2003/i=09/a=005

Abstract. Scenarios in which the knee of the cosmic ray spectrum depends on the particle rigidities usually predict that the cosmic ray composition becomes heavier above the knee and have associated a change in the spectral slope of each individual nuclear component which is steeper than the change ($\Delta\alpha \simeq 0.3$) observed in the total spectrum. We show that this implies that the very high energy ($E_\nu > 10^{14}$ eV) diffuse neutrino fluxes produced by cosmic rays hitting the atmosphere or colliding with the interstellar medium in the Galaxy will be significantly suppressed, making their detection harder but also reducing the background for the search for other (more challenging) astrophysical neutrino sources.

Keywords: cosmic rays, ultra high energy photons and neutrinos

JCAP 09(2003)005

 PII: S1475-7516(03)67928-0 1475-7516/03/090005+18$30.00

Contents

1. Introduction

The study of atmospheric neutrinos of sub-GeV and multi-GeV energies has been of paramount importance in the recent past, providing in particular the first clear evidence in favour of neutrino oscillations, and hence of non-vanishing neutrino masses. These neutrinos are produced mainly in the decay of pions and kaons (e.g. $\pi^- \to \mu^- \overline{\nu}_\mu$, with $\mu^- \to e^- \overline{\nu}_e \nu_\mu$) produced by the cosmic rays (CRs) hitting the upper atmosphere and generating air showers with a significant hadronic component. Due to the interplay between the mesons' decay and their interactions in the air, as the energy increases (with the associated relativistic dilation of their decay times) the mesons lose an increasing amount of energy before they decay, and also the muons produced can reach the ground before decaying. As a consequence of this, the predicted atmospheric neutrino spectrum becomes steeper than the CR spectrum typically by an extra power of the energy, with $\mathrm{d}N_\nu/\mathrm{d}E_\nu \propto E_\nu^{-3.7}$, while $\mathrm{d}N_{CR}/\mathrm{d}E_{CR} \propto E_{CR}^{-2.7}$ [1]–[3].

Comparing the charged mesons' decay length, $L \equiv \gamma c\tau$, where in particular $L_\pi \simeq 5.6$ km $(E_\pi/100$ GeV) and $L_K \simeq 7.5$ km (E_K/TeV), it is clear that above 100 GeV the pions traverse several attenuation lengths (corresponding to approximately 120 g cm^{-2}) in the atmosphere before decaying, and due to this the neutrino fluxes above a few hundred GeVs actually arise mainly from K decays. Kaons in turn are also significantly attenuated before decaying for energies above the TeV, with the effect that the prompt neutrinos from charmed particle decays become increasingly important.

Several groups have studied the charmed particle production by CRs [4]–[6], which actually requires us to take into account next to leading order (NLO) processes, which increase the charm production by more than a factor of two, and the cross sections are sensitive to the values of the partonic distribution functions at very small values of the scaling variable x, which introduces further uncertainties in the results, due to the need to extrapolate beyond the measured range. Even if the charmed mesons ($D^\pm$, D^0, D_s, $\Lambda_c, \ldots$) are produced at a rate $\sim 10^{-4}$ with respect to the non-charmed ones, their very short decay time, with $L_D \simeq 2$ km $(E_D/10$ PeV), implies that the

prompt neutrino spectral slope just follows the CR slope, and hence the prompt neutrinos eventually dominate the atmospheric neutrino fluxes above a PeV in the vertical direction, and somewhat above that energy at large zenith angles[3].

It is important at this point to take into account the fact that the primary CR spectrum shows a steepening at the so-called *knee*, corresponding to $E_{knee} \simeq 3 \times 10^{15}$ eV, with $\mathrm{d}N_{CR}/\mathrm{d}E_{CR} \propto E_{CR}^{-3}$ for $E_{CR} > E_{knee}$. The associated steepening in the induced neutrino fluxes has been obtained in the literature [4, 7], but these works usually assume for simplicity that the dominant CR component consists of protons, and only some crude attempts have been made to generalize these predictions to heavier compositions [6].

Another contribution to the diffuse neutrino fluxes produced by CRs is those resulting from the interactions of the CRs present all over the Galaxy with the ambient gas in the interstellar medium (ISM) [7]–[10]. The very low densities in the ISM ($n_{ISM} \simeq 1$ cm^{-3}) imply that essentially all mesons produced decay in this case without suffering any attenuation, and hence the neutrino fluxes are just the conventional ones from π, K and μ decays, and moreover their spectral slopes follow the behaviour of the primary CR spectrum. These neutrino fluxes are proportional to the column density of the ISM along the particular direction considered, and hence the flux is maximal in the direction to the galactic centre, it is generally enhanced near the galactic plane while it is minimum in the direction orthogonal to it.

Along directions near the plane of the Milky Way, these diffuse fluxes of galactic neutrinos may overcome the atmospheric neutrino background at energies larger than $\sim 10^{14}$ eV (the actual energy depends on the model adopted for charm production and on the assumed ISM column density, see below), but in the direction orthogonal to the plane they remain below the expected flux from prompt atmospheric neutrinos from charmed particle decays up to the highest energies [7]. Here again the usual simplifying working hypothesis is that the CR flux consists mainly of protons, and only crude attempts have been made to generalize the predictions to heavier compositions [9]. Although some works have found a strong sensitivity to the assumed composition both for atmospheric and galactic CR induced neutrinos, this issue is generally not treated appropriately and hence a more thorough analysis is required in order to estimate the neutrino fluxes with some confidence for $E_\nu > 10^{14}$ eV.

The very high energy neutrino fluxes produced by CRs both in the atmosphere and in the Galaxy are one of the important targets of present and future neutrino telescopes, such as AMANDA, BAIKAL, ANTARES, ICECUBE, etc. They are interesting *per se*, but they also represent the main background in the search for the fluxes arising from other potential neutrino sources, such as active galactic nuclei (AGNs) [11] and gamma ray bursts (GRBs) [12], which might give rise to detectable fluxes just in the energy range 10^{14}–10^{16} eV [13]. It is hence of primary importance to establish with some confidence the actual value of the CR induced neutrino fluxes, and the aim of the present work is to point out that the predictions are quite sensitive to the detailed composition and to the behaviour of the spectrum of the individual nuclear components of the CRs with energies above those corresponding to the knee in the spectrum.

A major problem that one has to face here is that, although the existence of the knee has been known for more than forty years, there is still no consensus on the underlying

[3] At large zenith angles the mesons produced high in the atmosphere are less affected by the attenuation before decay due to the fact that the atmosphere they traverse is more tenuous.

physics responsible for this feature, and different proposed explanations for it can lead to quite different predictions for the behaviour of the CR composition and the individual spectra. On the observational side, due to the indirect nature of the measurements, which are based on the analysis of extensive air showers, the situation is also far from settled.

A large class of possible scenarios to explain the knee is based on a rigidity dependent effect, such as a change in the CR acceleration efficiency at the sources [14]–[16] or on a change in the escape mechanism of CRs from the Galaxy [17]–[20], both of which, being magnetic effects, depend on the ratio E_{CR}/Z, where Z is the CR charge. Hence, in these scenarios the different nuclear components essentially steepen their spectra at an energy $E_Z \simeq ZE_{knee}$, and in this way the light components become more suppressed at smaller energies than the heavy ones. This leads to the prediction that the CR composition should become increasingly heavier above E_{knee}, in agreement with the latest observations of KASCADE [21] and the EAS-TOP/MACRO experiments [22]. In addition, the change in the spectral slope of each individual component usually turns out to be steeper than the change in slope of the total observed spectrum, which is $\Delta\alpha \simeq 3 - 2.7 = 0.3$. In particular, in the so-called diffusion/drift model [19, 20, 23, 24] in which the knee is due to a change in the escape mechanism of CRs from the Galaxy from one dominated by normal diffusion (with diffusion coefficient $D \propto E^{1/3}$) to one dominated by drift effects (with $D \propto E$), the spectral slope of each individual nuclear component changes by an amount $\Delta\alpha_Z \simeq 2/3$.

As we will show below, these rigidity dependent scenarios have a profound impact on the predictions of high energy diffuse neutrino fluxes, and hence a clear understanding of the physics responsible for the knee and also better measurements of air showers at these energies are crucial to predict the expected neutrino fluxes and to extract conclusions from them once they have been measured.

2. The cosmic ray spectrum

Figure 1 shows the observed cosmic ray differential spectrum from several experiments [25]. As mentioned above, the total CR spectrum is well described by power laws $\mathrm{d}N_{CR}/\mathrm{d}E_{CR} \propto E_{CR}^{-\alpha}$, with the spectral index changing from $\alpha \simeq 2.7$ to $\alpha \simeq 3$ at the so-called knee, occurring at $E_{knee} \simeq 3 \times 10^{15}$ eV. The CR spectrum turns harder again at the ankle, corresponding to $E_{ankle} \simeq 5 \times 10^{18}$ eV, a feature usually explained as the crossover between the dominance of the galactic CR component below the ankle and of the extragalactic one above it.

A simple way of describing the galactic CR flux within a rigidity dependent scenario is to assume that each galactic component of charge Z is given by

$$\frac{\mathrm{d}N_Z}{\mathrm{d}E} \equiv \phi_Z = \frac{\phi_Z^< \cdot \phi_Z^>}{\phi_Z^< + \phi_Z^>}, \tag{1}$$

where $\phi_Z^<$ ($\phi_Z^>$) is the CR flux below (above) the knee, and is given by

$$\left\{ \begin{array}{c} \phi_Z^< \\ \phi_Z^> \end{array} \right\} = f_Z \phi_0 \left(\frac{E}{E_0} \right)^{-\alpha_Z} \times \left\{ \begin{array}{c} 1 \\ (E/ZE_k)^{-\Delta\alpha} \end{array} \right\}. \tag{2}$$

In this expression, $\phi_0 = 3.5 \times 10^{-13}$ m^{-2} s^{-1} sr^{-1} eV^{-1} is the total CR flux at the reference energy E_0, hereafter taken as $E_0 = 1$ TeV, f_Z is the fractional CR abundance

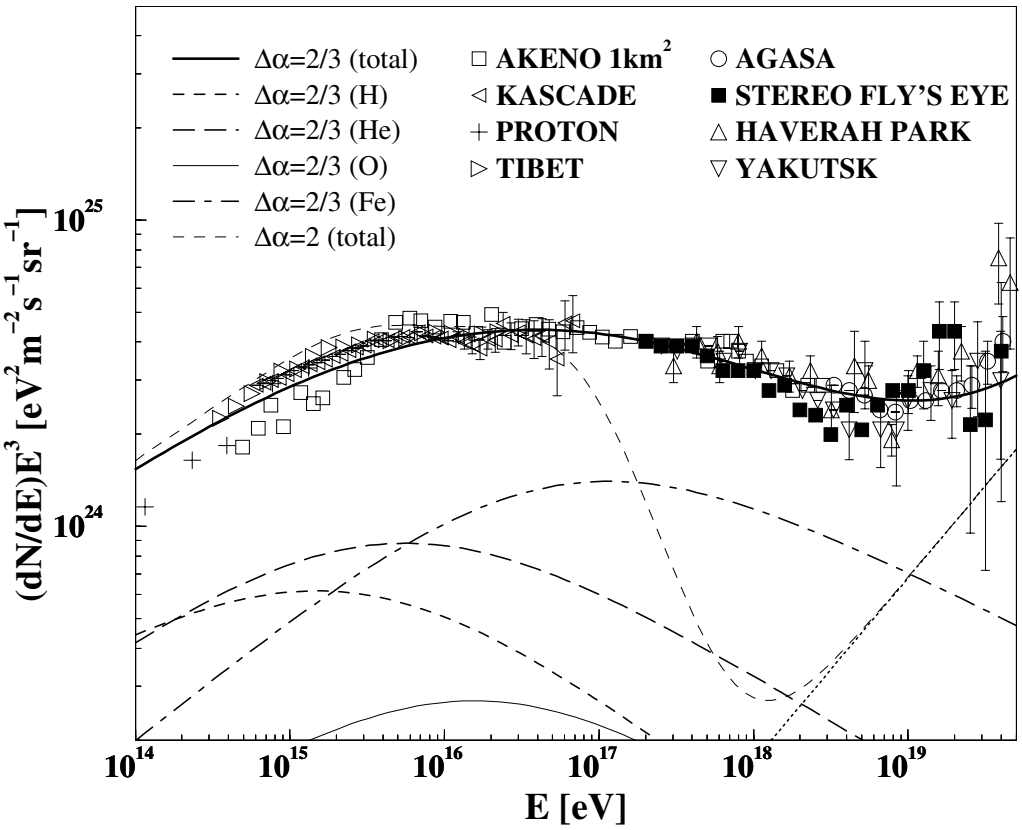

Figure 1. CR spectra obtained by considering rigidity-dependent scenarios parametrized according to equations (1) and (2). For the spectral index change $\Delta\alpha = 2/3$, the main contributions to the total flux, which correspond to nuclei of H, He, O and Fe, are also indicated. The dotted straight line corresponds to the extragalactic flux given by equation (3). Also shown are the relevant experimental observations.

at the same energy, α_Z is the low energy spectral index, $\Delta\alpha$ is the spectral index change across the knee (which is the same for all CR components) and E_k is a parameter that fixes the position of the knee, which is conveniently chosen to fit the observations. The expression in equation (1) provides then a smooth interpolation[4] between the flux $\phi_Z^<$ at low energies ($E < ZE_k$) and $\phi_Z^>$ at high energies ($E > ZE_k$). Also notice that the high-energy fluxes above the knee are extrapolated without considering upper cutoffs that could arise from a limiting energy achievable at the acceleration site. Little is known about this, but its inclusion would be straightforward. The CR abundances at $E = 1$ TeV and the low energy spectral indices are shown in table 1, and were taken from the data compiled in [26, 27].

[4] One may eventually generalize the expression in equation (1) as $\phi = \phi^< \cdot \phi^> / (\phi^{<n} + \phi^{>n})^{1/n}$, where the parameter n will control the 'width' of the knee, with $n \gg 1$ leading to an abrupt change in slope. We find, however, that $n = 1$ provides a very satisfactory fit to the CR data for the $\Delta\alpha = 2/3$ case considered.

Table 1. Cosmic ray fractional abundances (for $E = 1$ TeV) and low energy spectral indices from hydrogen to nickel.

Z	f_Z	α_Z	Z	f_Z	α_Z	Z	f_Z	α_Z	Z	f_Z	α_Z
1	0.3775	2.71	8	0.0679	2.68	15	0.0012	2.69	22	0.0049	2.61
2	0.2469	2.64	9	0.0014	2.69	16	0.0099	2.55	23	0.0027	2.63
3	0.0090	2.54	10	0.0199	2.64	17	0.0013	2.68	24	0.0059	2.67
4	0.0020	2.75	11	0.0033	2.66	18	0.0036	2.64	25	0.0058	2.46
5	0.0039	2.95	12	0.0346	2.64	19	0.0023	2.65	26	0.0882	2.59
6	0.0458	2.66	13	0.0050	2.66	20	0.0064	2.70	27	0.0003	2.72
7	0.0102	2.72	14	0.0344	2.75	21	0.0013	2.64	28	0.0043	2.51

For the extragalactic component, we will assume for definiteness that it consists of protons (this would anyhow only affect the predictions for $E_\nu > 10^{17}$ eV) and that it is given by

$$\left(\frac{\mathrm{d}N}{\mathrm{d}E}\right)_{XG} = 6.8 \times 10^{-34} \left(\frac{E}{10^{19}\ \mathrm{eV}}\right)^{-2.4} \ \mathrm{m}^{-2}\ \mathrm{s}^{-1}\ \mathrm{sr}^{-1}\ \mathrm{eV}^{-1}, \tag{3}$$

i.e. a flux similar to that considered in [24].

For the purpose of illustration, we display in figure 1 the cases of both $\Delta\alpha = 2/3$, corresponding to the diffusion/drift model (when a Kolmogorov spectrum of fluctuations is assumed for the random magnetic field component in which CR particles propagate [20, 23, 24]), and $\Delta\alpha = 2$, corresponding to an extreme model advocated in [27]. Figure 1 shows the fits that result from taking $\Delta\alpha = 2/3$ with the parameter value $E_k = 2.2 \times 10^{15}$ eV, and $\Delta\alpha = 2$ with $E_k = 3.1 \times 10^{15}$ eV. While the former exhibits an excellent agreement with the experimental observations, it can be seen that the latter shows an abrupt suppression above $\sim 10^{17}$ eV which results from the steep suppression of the different CR components above their knees [27], and due to this we will hereafter just focus on the $\Delta\alpha = 2/3$ case.

3. The flux of atmospheric neutrinos

The CR particles reaching the top of the atmosphere produce secondary fluxes of hadrons and leptons that are usually described by means of coupled cascade equations [2]–[5], which can be solved analytically under appropriate simplifying assumptions. In this work we will compute the fluxes of muon neutrinos and antineutrinos, which are the ones more readily detectable at underground detectors. At the energies considered, the neutrino flavour oscillations will have no effect on the atmospheric neutrinos, although they may be relevant for the neutrinos produced by CR interactions with the ISM (eventually redistributing in that case the produced ν_e and ν_μ fluxes evenly among the three flavours, something that can be incorporated into the final results straightforwardly).

The main contributions to the neutrino flux in the range of interest of this work (namely, for $E = 10^3$–10^8 GeV) arise, on the one hand, from the decay of the mesons $\pi^\pm, K^\pm, K^0_S$ and K^0_L, which produce the so-called conventional atmospheric neutrinos that dominate at low energies and, on the other hand, from the decay of the charmed mesons $D^0, D^\pm, \Lambda_c$ and D_s, which give rise to the so-called prompt charm neutrino flux that

dominates at very high energies. The muon contribution to the atmospheric neutrino flux is completely negligible in this context, since above $E \sim 10^3$ GeV the muons reach the ground and are stopped before decaying.

3.1. Nucleon and meson fluxes

The transport equation associated with a given cascade component j can be written as

$$\frac{\mathrm{d}\phi_j}{\mathrm{d}X}(E,X) = -\frac{\phi_j}{\lambda_j}(E,X) - \frac{\phi_j}{\lambda_j^d}(E,X) + \sum_k S_{kj}(E,X), \tag{4}$$

where, as usual, X is the slant depth, λ_j is the interaction length in air and λ_j^d is the decay length. Both characteristic lengths are measured in g cm^{-2} units (i.e. they include the factor $\rho(X)$ that corresponds to the local density of the atmosphere). Also notice that the decay length is linear in the energy due to the Lorentz time dilation factor, while the interaction length exhibits instead a much milder energy dependence. The last term in equation (4) corresponds to the production/regeneration term given by

$$S_{kj}(E,X) = \int_E^\infty \mathrm{d}E' \frac{\phi_k(E',X)}{\lambda_k(E')} \frac{1}{\sigma_{kA}(E)} \frac{\mathrm{d}\sigma_{kA\to j}(E,E')}{\mathrm{d}E}, \tag{5}$$

which actually couples the transport equations of different cascade components. Notice that σ_{kA} here refers to the total k+air cross section, while $\sigma_{kA\to j}$ corresponds to the process k+air $\to$ j+anything. Since the energies involved in the nuclear collisions between CRs and atmospheric nuclei are much higher than nuclear binding energies, only nucleon–nucleon interactions are relevant in this context. The different cascade components that we will take into account are hence N (that corresponds to the nucleon component in which protons and neutrons are grouped together) and $M = \pi^\pm$, $K^\pm$, K_L^0, D^0, $D^\pm$, Λ_c and D_s. As in [3], the K_S^0 can be considered as contributing to the pion flux. Moreover, we will assume for simplicity that the only non-negligible terms will be those corresponding to regeneration (i.e. S_{NN} and S_{MM}) and to meson production by nucleons (i.e. S_{NM}) [3, 4].

Let us consider in particular fluxes with the form $\phi_k(E,X) = E^{-\beta_k} g(X)$ (i.e. we consider the separation of variables in the fluxes, in which the energy dependent factor has a power-law behaviour). Then, it turns out that

$$S_{kj}(E,X) = \frac{\phi_k(E,X)}{\lambda_k(E)} Z_{kj}(E), \tag{6}$$

where Z_{kj} is the production/regeneration moment defined by

$$Z_{kj}(E) = \int_0^1 \mathrm{d}x\; x^{\beta_k - 1} \frac{1}{\sigma_{kA}(E)} \frac{\mathrm{d}\sigma_{kA\to j}(E,x)}{\mathrm{d}x}, \tag{7}$$

with $x \equiv E/E'$.

Assuming that the interaction lengths are energy independent and that the differential production distribution is Feynman scaling, the production/regeneration moments themselves become energy independent. Indeed, for the relevant interaction lengths and production/regeneration moments involving nucleons and non-charmed mesons, we consider the energy independent values given in [2, 3]. When necessary, we also take the β_k-dependence from fits to the data compiled and plotted in [2]. Moreover, following [5], the charm interaction lengths and regeneration moments are all set equal to the kaon ones.

For the production of charmed particles, however, one has to take into account the energy dependent moment given by equation (7), since the results are very sensitive to the particular cross section adopted for the charm production process. Indeed, the various estimates of the prompt atmospheric fluxes calculated so far are found to differ by almost two orders of magnitude [28].

Due to their relatively large mass, charmed quarks are usually considered to be produced in hard processes which can be well described by perturbative QCD (pQCD). To leading order (LO) in the coupling constant, the processes that contribute to the charm production cross section are the gluon–gluon fusion process $gg \to c\bar{c}$ and the quark–antiquark annihilation process $q\bar{q} \to c\bar{c}$. However, at the next to leading order (NLO) the gluon scattering process $gg \to gg$ shows up, giving a very significant contribution to the total cross section which increases it by a factor of $\sim$ 2–2.5 [29]–[31]. Concerning higher order corrections, their contribution is certainly small, since there are no qualitatively new channels opening up. Several parton distribution functions have been proposed and provide theoretical pQCD predictions that fit the available accelerator data reasonably well. However, in order to calculate the atmospheric charm flux the parton distribution functions need to be extrapolated to very small parton momentum fractions, typically corresponding to $x \simeq 4\ \mathrm{GeV}/E$ [6], which at the highest energies is well outside of the measured region ($x > 10^{-5}$), and the uncertainty in the extrapolation affects significantly the final results [5, 28]. In order to illustrate this uncertainty range, we display the results obtained with two different structure distribution functions, namely the CTEQ3 parton distribution function [32] and the Golec-Biernat, Wüsthoff (GBW) model [33], which includes gluon saturation effects. The corresponding charm production cross sections were obtained either directly from the fit given in [6] (for the results based on the GBW saturation model), or by fitting the results given in figure 4 of [5] for the CTEQ3 structure functions set with $M = 2m_c = 2\mu$, with the charm mass $m_c = 1.3$ GeV, and interpolating the results for different energies. For the nucleon–air cross section, we used the parametrization given by [34]

$$\sigma_{NA}(E) = \left[280 - 8.7 \ln\left(\frac{E}{\mathrm{GeV}}\right) + 1.14 \ln^2\left(\frac{E}{\mathrm{GeV}}\right)\right]\ \mathrm{mb}. \tag{8}$$

Once all relevant interaction lengths and production/regeneration moments are determined, the nucleon and meson atmospheric fluxes can be calculated from the coupled cascade equations given by (4) and (6). Recalling that these expressions were obtained under the assumption of power-law nucleon and meson spectra, we will first discuss the results for an initial nucleon flux given according to $\phi_N(E, X = 0) = \phi_{0N} E^{-\gamma}$, discussing the general case further below.

Under the assumptions mentioned above, the nucleon flux develops independently from the meson fluxes and is given by

$$\phi_N(E, X) = \mathrm{e}^{-X/\Lambda_N} \phi_{0N} E^{-\gamma}, \tag{9}$$

where the nucleon attenuation length is defined as

$$\Lambda_N = \frac{\lambda_N}{1 - Z_{NN}}. \tag{10}$$

Concerning the meson cascade equations, they are usually solved by considering separately the low energy solution ϕ_M^L (which neglects the interaction and regeneration

terms, since $\lambda_M \gg \lambda_M^d$ at low energies) and the high energy solution ϕ_M^H (which neglects instead the decay term, since $\lambda_M \ll \lambda_M^d$ at very high energies) [2]–[4].

The high energy solution is given by

$$\phi_M^H(E,X) = \frac{Z_{NM}}{1-Z_{NN}} \frac{\mathrm{e}^{-X/\Lambda_M} - \mathrm{e}^{-X/\Lambda_N}}{1-\Lambda_N/\Lambda_M} \phi_{0N} E^{-\gamma}, \tag{11}$$

where the meson attenuation length Λ_M is defined analogously to equation (10).

For the low energy case, the solution is obtained by replacing $\Lambda_M \to \lambda_M^d$ in the last equation. Recalling that $\lambda_M^d \propto E$, the resulting expression couples the dependence on the energy and the slant depth, and hence it does not lead to just a simple power law energy spectrum. However, for not very small values of X the solution reduces to

$$\phi_M^L(E,X) = \frac{Z_{NM}}{1-Z_{NN}} \frac{\lambda_M^d}{\Lambda_N} \mathrm{e}^{-X/\Lambda_N} \phi_{0N} E^{-\gamma}. \tag{12}$$

In equations (9)–(12), Z_{NN}, Z_{NM} and Z_{MM} are to be evaluated for the nucleon spectral index γ. Notice also that the high energy meson flux has the same spectral index as the nucleon flux, while the low energy meson solution is flatter by an extra power of the energy, due to the energy dependence implicit in λ_M^d.

3.2. Neutrino flux

The neutrino flux produced via the meson weak decay can be calculated following the same scheme described above for the atmospheric nucleon and meson fluxes. Indeed, the neutrino flux is given by a transport equation analogous to equation (4), but actually much simpler since it contains only the source terms arising from meson decay, i.e.

$$\frac{\mathrm{d}\phi_\nu}{\mathrm{d}X}(E,X) = \sum_M S_{M\nu}(E,X), \tag{13}$$

where

$$S_{M\nu}(E,X) = \int_E^\infty \mathrm{d}E' \frac{\phi_M(E',X)}{\lambda_M^d(E')} \frac{1}{\Gamma_M(E)} \frac{\mathrm{d}\Gamma_{M\nu}(E,E')}{\mathrm{d}E}. \tag{14}$$

The decay distribution can be put in terms of $F_{M\nu}$, the inclusive neutrino spectrum in the decay of meson M, by means of the relation

$$\frac{1}{\Gamma_M(E)} \frac{\mathrm{d}\Gamma_{M\nu}(E,E')}{\mathrm{d}E} = B_{M\nu} F_{M\nu}(E,E'), \tag{15}$$

where $B_{M\nu}$ is the branching ratio for the decay of meson M into a state with the given neutrino ν. In the ultrarelativistic limit, the inclusive neutrino spectrum scales as $F_{M\nu}(E,E') = F_{M\nu}(E/E')/E'$ [2, 3]. Moreover, we have already derived the asymptotic solutions for the meson fluxes, which are of the form $\phi_M(E,X) \propto E^{-\beta} g(X)$, with $\beta = \gamma$ ($\beta = \gamma - 1$) for the high (low) energy fluxes (see equations (11) and (12)). Thus, the source terms given by equation (14) can be rewritten as

$$S_{M\nu}(E,X) = \frac{\phi_M(E,X)}{\lambda_M^d(E)} Z_{M\nu}^{\beta+1}(E), \tag{16}$$

where the β-dependent meson decay moments are defined by[5]

$$Z^{\beta}_{M\nu}(E) = B_{M\nu} \int_0^1 \mathrm{d}x\; x^{\beta-1} F_{M\nu}(x). \tag{17}$$

The decay moments used in this work were calculated by fitting the β-dependence of the relevant moments tabulated in [4] for $2.7 \leq \beta \leq 4$, which were determined with Lund Monte Carlo simulation programs.

Then the asymptotic low and high energy neutrino fluxes can be determined from equations (13) and (16), which involve the meson decay moments and the corresponding high and low energy meson fluxes derived in equations (11) and (12). The low energy solution reads

$$\phi^{L}_{\nu}(E, X) = Z^{\gamma}_{M\nu} \frac{Z_{NM}}{1 - Z_{NN}} \left(1 - \mathrm{e}^{-X/\Lambda_N}\right) \phi_{0N} E^{-\gamma}. \tag{18}$$

As expected, the neutrino flux develops rapidly, on the scale of a nucleon interaction length, and then remains stable. Hence, at ground level ($X \gg \Lambda_N$) the low energy flux will be

$$\phi^{L}_{\nu}(E) = Z^{\gamma}_{M\nu} \frac{Z_{NM}}{1 - Z_{NN}} \phi_{0N} E^{-\gamma}. \tag{19}$$

Similarly, the high energy flux at ground is

$$\phi^{H}_{\nu}(E) = Z^{\gamma+1}_{M\nu} \frac{Z_{NM}}{1 - Z_{NN}} \frac{\ln\left(\Lambda_M/\Lambda_N\right)}{1 - \Lambda_N/\Lambda_M} \frac{\epsilon_M}{\cos\theta} \phi_{0N} E^{-(\gamma+1)}, \tag{20}$$

where θ is the zenith angle of the CR incidence direction considered and

$$\epsilon_M = \frac{m_M c h_0}{\tau_M}, \tag{21}$$

with m_M and τ_M the meson's mass and mean life, respectively, and $h_0 = 6.4$ km a typical scale height for density variations in the atmosphere. Since the production/regeneration moments Z_{NN}, Z_{NM} and Z_{MM} are the same as those appearing in the meson fluxes, they are to be evaluated for the nucleon spectral index γ. Equation (20) is actually valid for zenith angles sufficiently small so that the curvature of the Earth can be neglected, and assumes a density profile of an isothermal atmosphere (i.e. $\rho(h) \propto \exp(-h/h_0)$), which is appropriate in the stratosphere ($h \geq 11$ km) where most particle interactions occur [3, 4]. For very large angles, one can still use equation (20) with the simple prescription of replacing $\theta \to \theta^*(\theta, h = 30\ \mathrm{km})$, where for a given line of sight that corresponds to an angle θ at the observer's position, the angle $\theta^*(\theta, h)$ is the zenith angle that would be observed at a location where this same line of sight is at a height h with respect to the ground [3]. For instance, for CRs incident in the horizontal direction ($\theta = 90°$), one has that $\theta^* \simeq \arcsin(1 + h/R_{\oplus})^{-1} \simeq 84.5°$.

In order to obtain a general expression for the atmospheric neutrino fluxes deep in the atmosphere, the asymptotic solutions given by equations (19) and (20) can be joined together by means of the interpolation function

$$\phi_{\nu} = \frac{\phi^{L}_{\nu} \cdot \phi^{H}_{\nu}}{\phi^{L}_{\nu} + \phi^{H}_{\nu}}, \tag{22}$$

[5] The branching ratio is here included in the definition of the decay moments, in analogy with the production/regeneration moments that include the multiplicity of the final states. This coincides with [4] but differs from [3].

which is actually analogous to the interpolation function given in equation (1) to join the fluxes associated with each galactic CR component below and above their knees.

We have described so far a calculational scheme that provides the nucleon, meson and neutrino fluxes produced by an initial power law nucleon flux $\phi_N(E, X = 0) = \phi_{0N} E^{-\gamma}$ hitting the top of the atmosphere. We now seek the corresponding results for the full CR spectrum arriving at the Earth, taking into account both the CR composition and the break in the CR spectra at the knee. Let ϕ_Z be the CR flux associated with the CR component of nuclei of charge Z and mass Am_N (with A being the average mass number corresponding to element Z). This nuclear component provides a nucleon flux $\phi_{N,Z}$ given by $\phi_{N,Z}(E_N) = A\phi_Z(E = AE_N)$. If the flux of the CR component of charge Z is $\phi_Z(E) = \phi_{0Z}(E/E_0)^{-\gamma_Z}$, the corresponding nucleon flux is then given by

$$\phi_N(E) = \sum_Z A^{2-\gamma_Z} \phi_{0Z} \left(\frac{E}{E_0}\right)^{-\gamma_Z}. \tag{23}$$

From these considerations, the procedure to calculate the neutrino flux produced by the galactic CR flux parametrized by equations (1) and (2) is now straightforward. Indeed, the CR component of charge Z is represented by two power law fluxes $\phi_Z^<$ and $\phi_Z^>$, with spectral indices α_Z and $\alpha_Z + \Delta\alpha$, respectively. For each power law flux, we can compute the corresponding nucleon flux given by equation (23) and use it to calculate the associated neutrino flux. Then, the final neutrino flux produced by the given CR component can be obtained by interpolating the two solutions, using again the interpolation function analogous to equation (1). Finally, the total neutrino flux results from summing over the contribution of all galactic CR components together with the additional contribution from the extragalactic component given by equation (3).

Figure 2 shows the atmospheric neutrino fluxes that correspond to the $\Delta\alpha = 2/3$ rigidity dependent scenario, with the parametrization formulae and parameter values given in section 2. The figure shows the contribution coming from different components and for different cases, namely the vertical and horizontal conventional, prompt charm/GBW and prompt charm/CTEQ3 fluxes. For the prompt charm flux calculated with the GBW model, the figure also shows the total vertical and horizontal neutrino fluxes. Finally, in the latter case the conventional, charm and total neutrino fluxes produced by the extragalactic CR component are also indicated. As is clear from equation (23), the induced neutrino fluxes are sensitive, on the one hand, to the CR composition assumed and, on the other hand, to the model assumed to reproduce the steepening of the CR spectrum at the knee. Previous works that have taken the knee into account have assumed for simplicity that the dominant CR component consists of protons alone, having a spectral change $\Delta\alpha = 0.3$ at E_{knee}.

In order to observe the effect of the CR composition on the neutrino fluxes, figure 3 compares the total horizontal atmospheric fluxes (with the prompt charm component calculated with the GBW model) as obtained for different assumptions on the CR spectrum, namely the $\Delta\alpha = 2/3$ rigidity dependent scenario (that corresponds to the results given already in figure 2), the same total CR spectrum but assuming it consists only of protons, and the CR spectrum used in [4, 7] (which is assumed to be constituted by protons and has a single spectral index change of $\Delta\alpha = 0.3$ at $E_{knee} = 5 \times 10^{15}$eV). The latter CR spectrum has a normalization which is lower by a factor of ~ 2.6 compared to the former ones, and indeed it seems to lay somewhat below the present observational

JCAP 09(2003)005

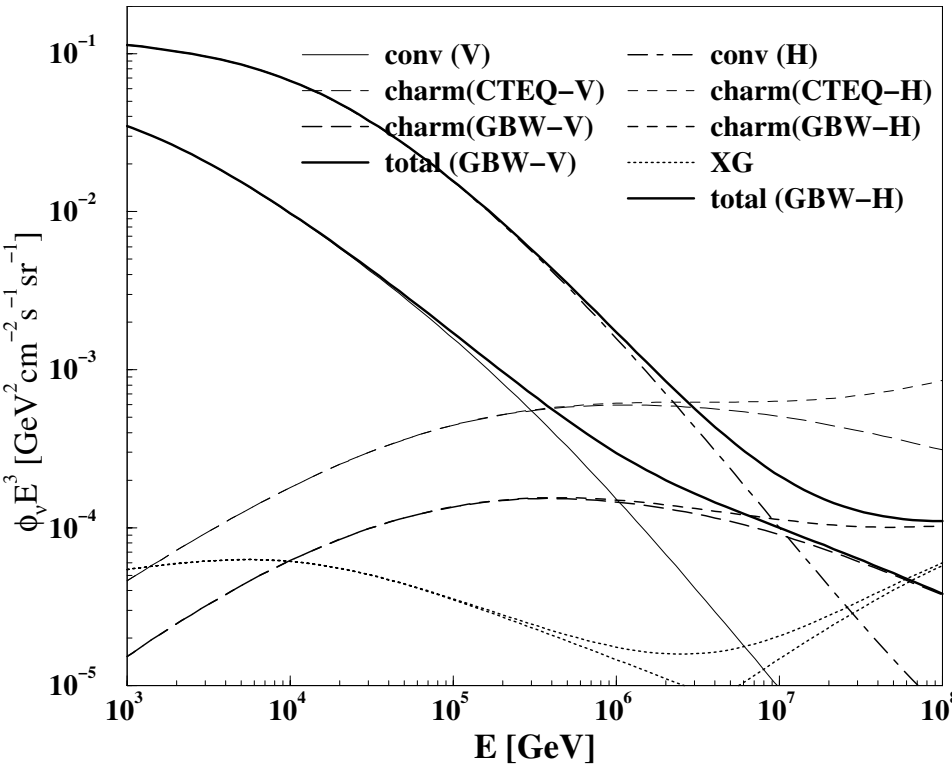

Figure 2. Atmospheric ($\nu_\mu + \bar{\nu}_\mu$) fluxes for the $\Delta\alpha = 2/3$ rigidity dependent scenario (that corresponds to the CR spectrum plotted in figure 1). The vertical and horizontal conventional, prompt charm/GBW and prompt charm/CTEQ3 fluxes are shown, as well as the total vertical and horizontal neutrino fluxes for prompt charm/GBW. In the latter case, the conventional, charm and total neutrino fluxes produced by the extragalactic CR component are also indicated.

JCAP 09(2003)005

data. Comparing the results for the same total CR spectrum, one can observe that the neutrino flux corresponding to the composition of different nuclear species is clearly below that produced by a CR spectrum formed only by protons, and also that this effect is more significant at higher energies. Indeed, equation (23) shows that the nuclear CR component of charge Z and mass A gives a contribution to the nucleon flux which is suppressed by a factor of $A^{2-\alpha_Z} \sim A^{-0.7}$ below the respective knee, while it becomes suppressed by a factor $A^{2-\alpha_Z-\Delta\alpha} \sim A^{-1.4}$ well above it. This effect was not appropriately treated in [6], where the suppression was considered to be given by a factor of A^{-2}, and moreover the impact of the change in the composition at the knee was never discussed before. The strong suppression of the ν flux produced by the heavier components implies that the light (H and He) components are still responsible for a large fraction of the neutrinos above their knee, and hence the change in slope of the individual components is also reflected in the change in slope of the neutrino fluxes.

Finally, let us comment briefly on the effect of assuming upper cutoffs in the galactic CR high energy fluxes above the knee. Indeed, the different nuclear components may have upper cutoffs at the energies $E_{cZ} \simeq ZE_c$, where E_c would correspond to the cutoff of the

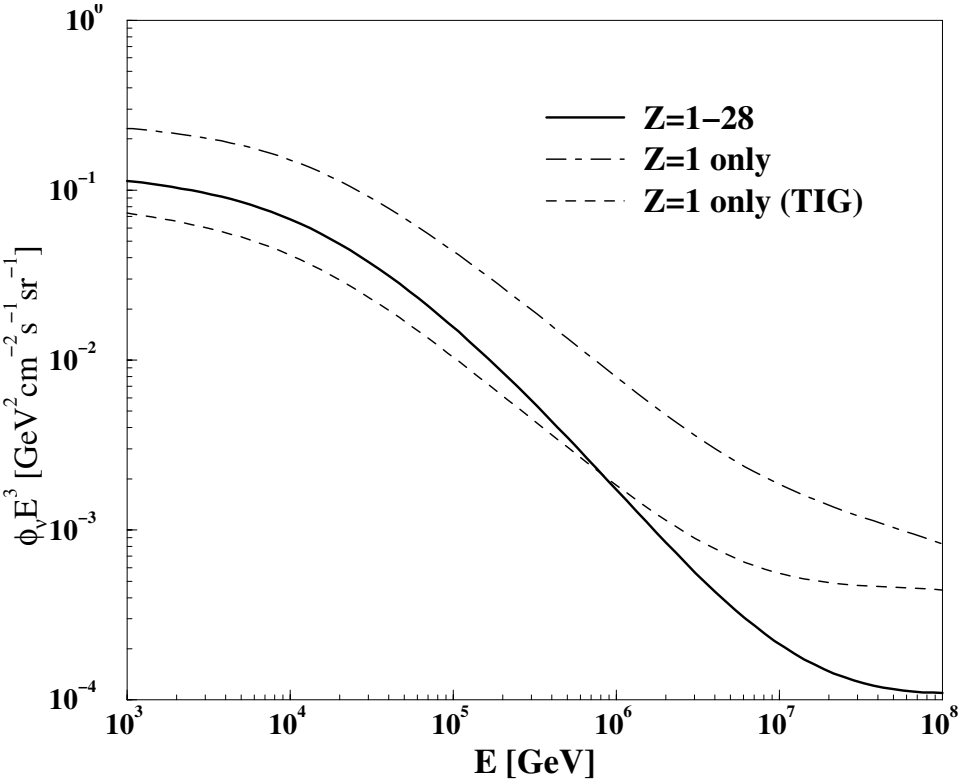

Figure 3. Comparison of the total horizontal atmospheric ($\nu_\mu + \bar{\nu}_\mu$) flux for prompt charm/GBW produced by CRs under different assumptions concerning spectrum and composition: the $\Delta\alpha = 2/3$ rigidity dependent scenario that considers the contribution of CR components with charge $1 \leq Z \leq 28$; the same total CR spectrum but assuming it consists only of protons; and the CR spectrum used in [4, 7] (TIG), which also takes only protons into account but has a lower normalization.

proton component. In that case, the CR composition above E_c would become increasingly heavier than the one considered here, and hence the associated neutrino flux suppression would become enhanced up to the high energy region in which the extragalactic component dominates. In the context of the supernova paradigm for the origin of galactic cosmic rays, this upper cutoff may range between $E_c \simeq 10^{15}$ and 10^{17} eV, depending on whether the strong shocks develop in the ISM or in the stellar wind of the predecessor star or that of a companion [35]. For electrostatic acceleration in a young pulsar the limiting energy may be even higher.

4. The flux of galactic neutrinos

The neutrino fluxes produced during the propagation of the CR particles through the ISM can be determined following the procedure described in the preceding section for the production of atmospheric neutrinos. For simplicity, we consider that the CRs are distributed homogeneously within the galactic disk. The highly relativistic CR particles

interact with the ambient gas in the ISM, which is a very low density, non-relativistic plasma constituted chiefly by atomic and molecular hydrogen that can be described by an homogeneous nucleon density $n_{ISM} \simeq 1$ cm^{-3} [36]. The treatment follows essentially the same considerations described above, but in this case one has to consider that the interaction of the secondaries produced in the nucleon–nucleon interactions is completely negligible due to the extremely low ISM densities, which allows for their decay well before interactions can take place, irrespective of the energy considered. Hence, the main contributions to the diffuse neutrino flux produced in the Galaxy arise from the decay of pions and muons, while the additional contributions coming from production and decay of heavier mesons can be safely disregarded.

As in the preceding section, let us first consider an initial nucleon flux given by $\phi_N(E, X = 0) = \phi_{0N} E^{-\gamma}$. Notice that in this context the atmospheric slant depth should be replaced by the ISM column density traversed along the line of sight (i.e. $X \to R m_N n_{ISM}$, where R is the distance measured from the border of the galactic disk along the line of sight). Due to the extreme faintness of the ISM, we should now take into account that[6] $X \ll \lambda_N$. Indeed, it turns out that

$$\frac{X}{\lambda_N} = 3.1 \times 10^{-6} \left(\frac{R}{\text{kpc}}\right) \left(\frac{\sigma_{NN}}{\text{mb}}\right), \tag{24}$$

where the nucleon–nucleon total cross section is

$$\sigma_{NN} \simeq \left[35.49 + 0.307 \ln^2 \left(s/28.94 \text{ GeV}^2\right)\right] \text{ mb}, \tag{25}$$

and where $s \simeq 2 m_N E$ stands for the centre of mass energy squared [37].

Hence, considering equation (18) with $X \ll \lambda_N$, the neutrino flux produced from pion decay in the ISM is

$$\phi_\nu(E, X) = Z^\gamma_{M\nu} Z_{NM} \frac{X}{\lambda_N} \phi_{0N} E^{-\gamma}. \tag{26}$$

In order to determine the muon decay contribution, it suffices to estimate it directly from the results obtained already for pion decay. From the decay kinematics, the mean fraction of energy (relative to the parent particle) in the $\pi \to \mu + \nu_\mu$ decay is $K_\pi = 0.21$ for the ν_μ and 0.79 for the muon [1]. Analogously, in the $\mu \to e + \nu_e + \nu_\mu$ decay the effective fraction of energy for the resulting ν_μ is 0.35 [1], i.e. a fraction $K_\mu = 0.28$ relative to the original pion. Hence, one expects a muon decay contribution approximately a factor $(K_\mu/K_\pi)^\gamma$ larger than the neutrino flux from pion decay (for instance, a factor of 2.1 for a nucleon spectral index $\gamma = 2.7$, in reasonable agreement with more detailed calculations [7]).

As commented on above, the galactic neutrino flavour oscillations may redistribute the produced ν_μ and ν_e fluxes evenly among the three flavours. In that case, the calculation of the electron neutrino flux produced by CR interactions with the ISM is also required in order to determine the galactic muon neutrino flux reaching the Earth. This flux is mainly produced in the $\mu \to e + \nu_e + \nu_\mu$ decay, in which the effective fraction of energy for the ν_e is 0.3 [1]. Thus, the ν_e flux is approximately a factor $(0.3/0.35)^\gamma$ times the

[6] In this case, λ_N corresponds to the interaction length for nucleons propagating through the ISM. Notice that λ_N, expressed in g cm^{-2}, is actually very similar to the one corresponding to nucleon propagation in air. In contrast, the meson decay length λ^d_M, which is linear in the mass density of the medium, will be much smaller in the ISM than in the atmosphere.

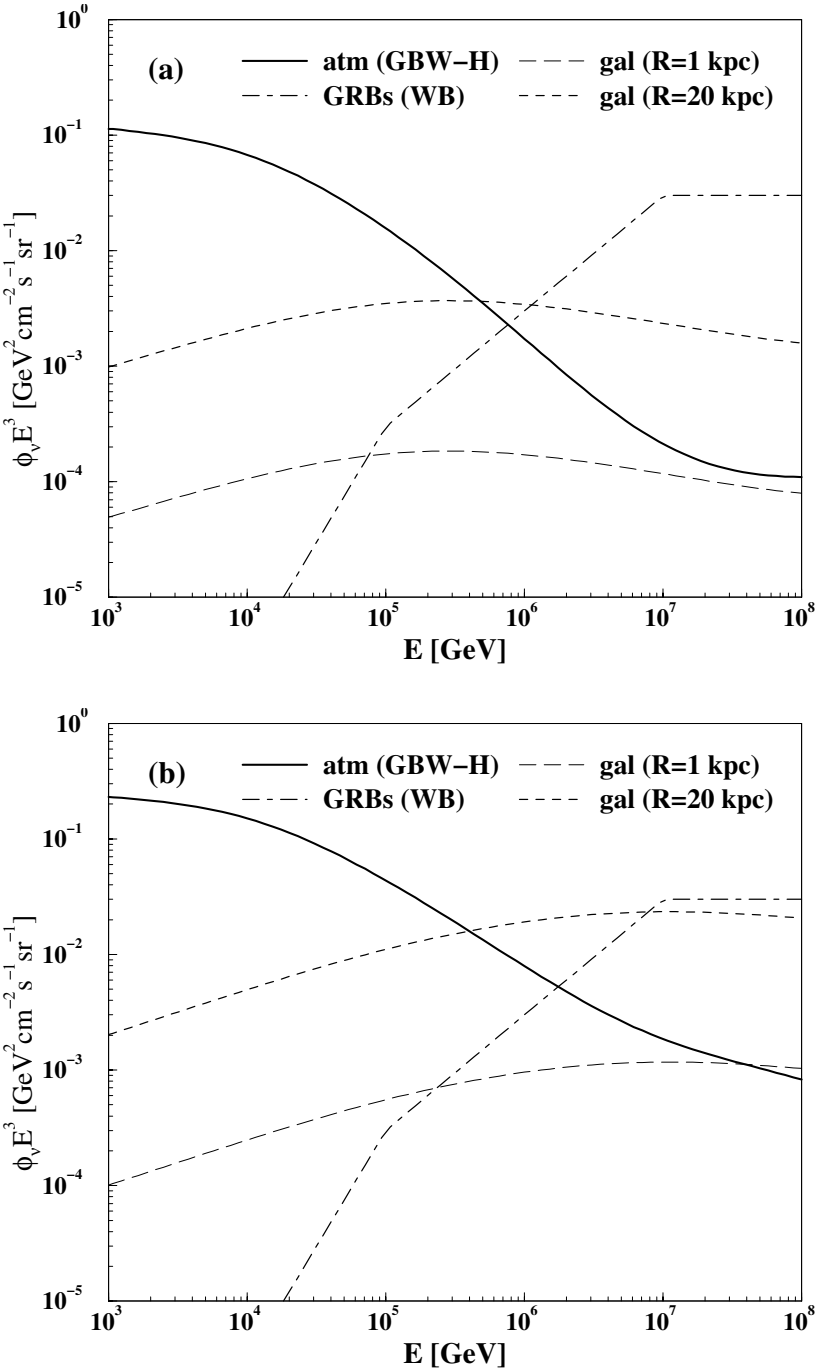

Figure 4. Neutrino fluxes ($\nu_\mu + \bar{\nu}_\mu$) produced by CRs in the ISM (for different path lengths traversed through the ISM, namely $R = 1$ and 20 kpc) and in the atmosphere (for the horizontal direction, using the GBW model for the prompt charm contribution) assuming different CR compositions: (a) the $\Delta\alpha = 2/3$ rigidity dependent scenario that considers the contribution of CR components with $1 \leq Z \leq 28$; (b) the same total CR spectrum but assuming it consists only of protons. For comparison, the Waxman–Bahcall predictions for the astrophysical diffuse neutrino fluxes produced in their model of GRBs are also shown.

JCAP 09(2003)005

ν_μ flux produced in the muon decay (i.e. a factor of ~ 0.7 for a nucleon spectral index $\gamma = 2.7$, again in good agreement with previous, more detailed calculations [7]). Hence, if the neutrino flavours are redistributed by oscillations, the $(\nu_\mu + \bar{\nu}_\mu)$ galactic flux will be a factor $(1 + 0.7 \times 2.1/3.1)/3 \simeq 1/2$ of that depicted in figure 4, which neglects the neutrino oscillations.

In order to calculate the galactic neutrino flux induced by the full CR spectrum, the procedure follows the same steps already described above for the atmospheric fluxes. The total galactic neutrino fluxes are shown in figure4(a) for $R = 1$ and 20 kpc, and correspond to the $\Delta\alpha = 2/3$ rigidity dependent scenario (with the same parametrization used for the previous figures and detailed in section 2). For comparison, the figure also shows the total atmospheric neutrino flux in the horizontal direction with the prompt charm component calculated using the GBW model, as well as the Waxman–Bahcall flux predictions for the astrophysical diffuse neutrino fluxes produced in their model of GRBs [12, 13]. Analogously, figure4(b) shows the results corresponding to the same total CR spectrum but assuming it to consist only of protons. In agreement with previous results [7], we observe that the galactic flux in the direction orthogonal to the plane (corresponding for instance to $R = 1$ kpc) remains below the atmospheric flux up to the highest energies. Along directions near the galactic plane (e.g. for $R = 20$ kpc), the flux of galactic neutrinos produced in the ISM instead overcomes the atmospheric flux at energies larger than $\sim 10^{14}$ eV. The energy at which the galactic flux actually dominates depends to a large extent on the particular model adopted for charm production, as discussed above, and the results naturally also vary according to the assumed ISM column density and the zenith angle of arrival direction in the atmosphere. These figures show very clearly the significant effect of suppression in the neutrino fluxes that results from considering a rigidity dependent scenario. Indeed, above $\sim 10^{15}$ eV the Waxman–Bahcall flux is found to overcome the background of galactic neutrinos with trajectories nearly contained in the galactic plane. However, if the same total CR spectrum is taken to be formed by protons alone, the resulting background flux of galactic neutrinos turns out to be larger than the Waxman–Bahcall flux up to $\sim 10^{16}$ eV, and then both fluxes stay with comparable magnitude up to the highest energies. Hence, rigidity dependent scenarios result in a significantly reduced background for the search for astrophysical neutrino sources of current interest, such as for instance GRBs or AGNs.

5. Conclusions

We computed in this work the high energy diffuse fluxes of muon neutrinos (and antineutrinos) produced by CRs hitting the upper atmosphere or interacting with the ISM in the Galaxy, showing that the results are quite sensitive to both the total CR spectrum and the CR composition assumed. Concerning the former, we compared previous results (which adopted an overall normalization for the CR spectrum actually somewhat below present observational data, and a single and abrupt slope change representing the knee) with those obtained from considering a smooth CR spectrum that soundly fits the observations and reproduces its main relevant features (namely, the knee, the second knee and the ankle). With respect to the latter, we showed that taking into account a CR composition that turns heavier above the knee (i.e. in agreement with the scenarios that explain the knee as due to a rigidity dependent effect) the induced neutrino fluxes

become significantly suppressed, thus making their detection harder but also reducing the background for the search of other astrophysical neutrino sources. In particular, we compared our results with the Waxman–Bahcall predictions for the neutrino fluxes produced in their model of GRBs, and found indeed that the signal-to-background ratio for this model becomes significantly enhanced when considering a CR composition with the contribution of different nuclear species, as opposed to the case in which the full CR spectrum is assumed to be composed of protons alone. An analogous effect would lower the neutrino flux produced by the extragalactic component (which gives the dominant contribution to the total neutrino flux above $E \sim 10^{17}$ eV) if it were not constituted just by protons, as we assumed here. It is then clear that if the diffuse neutrino fluxes predicted in the GRBs models [12] or the even larger ones associated with some AGN models [11] do actually exist, the observation of atmospheric or galactic CR induced neutrino fluxes above 10^{14} eV will probably remain hopeless. Let us also mention that the detection of these astrophysical fluxes is already challenging for the next generation of neutrino telescopes, such as ICECUBE [13], and hence the detection of the CR neutrino backgrounds in the case that other astrophysical diffuse fluxes were absent would be still further ahead into the future.

It may also be of interest to consider the atmospheric muon fluxes produced by CRs. For instance, it has recently been suggested [28] that the observation of the down-going atmospheric muons with neutrino telescopes would provide an indirect measure of the prompt atmospheric neutrino flux, and hence this could be used to confront the NLO QCD predictions. Indeed, due to the charmed particle semileptonic decay kinematics, it turns out that the prompt muon flux coincides with the prompt neutrino flux to within $\sim 10\%$, irrespective of the energy and independently of the model used to treat the atmospheric charm production [28]. On the other hand, the atmospheric conventional muon flux is about a factor of ~ 5 larger than the conventional muon neutrino flux within the energy range of interest of this work, and exhibits roughly the same energy dependence [28]. Completely analogous effects to those described here for the neutrino fluxes should then be expected for the atmospheric muons produced by CRs reaching the Earth.

Finally, we stress the key importance of determining confidently the CR composition around and above the knee, since it appears in this context as decisive in order to estimate reliably the diffuse high energy neutrino background produced by CRs. Moreover, solving the CR composition puzzle will also provide a valuable means of testing the different proposals concerning the origin and nature of the knee, and will thus shed new light on this long standing problem.

Acknowledgment

Work supported by CONICET and Fundación Antorchas, Argentina.

References

[1] Volkova L V, 1980 *Yad. Fiz.* **31** 1510 [SPIRES]
Volkova L V, 1980 *Sov. J. Nucl. Phys.* **31** 784 [SPIRES] (translation)
[2] Gaisser T K, 1990 *Cosmic Rays and Particle Physics* (Cambridge: Cambridge University Press)
[3] Lipari P, 1993 *Astropart. Phys.* **1** 195 [SPIRES]
[4] Thunman M, Ingelman G and Gondolo P, 1996 *Astropart. Phys.* **5** 309 [SPIRES]

[5] Pasquali L, Reno M H and Sarcevic I, 1999 *Phys. Rev.* D **59** 034020 [SPIRES]
[6] Martin A D, Ryskin M G and Staśto A M, 2003 *Acta Phys. Polon.* **B34** 3273 [SPIRES]
[7] Ingelman G and Thunman M, 1996 *Preprint* hep-ph/9604286
[8] Stecker F W, 1979 *Astrophys. J.* **228** 919 [SPIRES]
[9] Domokos G, Elliott B and Kovesi-Domokos S, 1993 *J. Phys. G: Nucl. Part. Phys.* **19** 899 [SPIRES]
[10] Berezinskii V S *et al*, 1993 *Astropart. Phys.* **1** 281 [SPIRES]
[11] Stecker F W and Salamon M H, 1996 *Space Sci. Rev.* **75** 341
[12] Waxman E and Bahcall J, 1999 *Phys. Rev.* D **59** 023002 [SPIRES]
[13] Ahrens J *et al* (IceCube Collaboration), 2003 *Preprint* astro-ph/0305196
[14] Fichtel C E and Linsley J, 1986 *Astrophys. J.* **300** 474 [SPIRES]
[15] Jokipii J R and Morfill G E, 1986 *Astrophys. J.* **312** 170 [SPIRES]
[16] Kobayakawa K, Honda Y S and Samura T, 2002 *Phys. Rev.* D **66** 083004 [SPIRES]
[17] Syrovatsky S I, 1971 *Commun. Astrophys. Space Phys.* **3** 155
[18] Wdowczyk J and Wolfendale A W, 1984 *J. Phys. G: Nucl. Phys.* **10** 1453
[19] Ptuskin V S *et al*, 1993 *Astron. Astrophys.* **268** 726 [SPIRES]
[20] Candia J, Roulet E and Epele L N, 2002 2002 *J. High Energy Phys.* JHEP12(2002)033 [SPIRES]
[21] Kampert K-H *et al* (KASCADE Collaboration), 1999 *Proc. 26th Int. Cosmic Ray Conf. (Salt Lake City, UT, 1999)* OG.1.2.11
Kampert K-H *et al* (KASCADE Collaboration), 2001 *Preprint* astro-ph/0102266
[22] Aglietta M *et al* (EAS-TOP and MACRO Collaborations), 2003 *Preprint* astro-ph/0305325
[23] Candia J, Mollerach S and Roulet E, 2002 2002 *J. High Energy Phys.* JHEP12(2002)032 [SPIRES]
[24] Candia J, Mollerach S and Roulet E, 2003 2003 *J. Cosmol. Astropart. Phys.* JCAP05(2003)003 [SPIRES]
[25] Nagano M and Watson A A, 2000 *Rev. Mod. Phys.* **72** 689 [SPIRES]
[26] Wiebel-Sooth B and Biermann P L, 1998 *Astron. Astrophys.* **330** 389 [SPIRES]
[27] Hörandel J R, 2003 *Astropart. Phys.* **19** 193 [SPIRES]
[28] Gelmini G, Gondolo P and Varieschi G, 2003 *Phys. Rev.* D **67** 017301 [SPIRES]
[29] Nason P, Dawson S and Ellis R K, 1988 *Nucl. Phys.* B **303** 607 [SPIRES]
[30] Beenakker W *et al*, 1989 *Phys. Rev.* D **40** 54 [SPIRES]
[31] Matsuura T, van der Marck S C and van Neerven W L, 1989 *Nucl. Phys.* B **319** 570 [SPIRES]
[32] Lai H *et al* (CTEQ Collaboration), 1995 *Phys. Rev.* D **51** 4763 [SPIRES]
[33] Golec-Biernat K J and Wüsthoff M, 1999 *Phys. Rev.* D **59** 014017 [SPIRES]
Bartels J, Golec-Biernat K J and Kowalski H, 2002 *Phys. Rev.* D **66** 014001 [SPIRES]
[34] Mielke H H *et al*, 1994 *J. Phys. G: Nucl. Part. Phys.* **20** 637 [SPIRES]
[35] Biermann P L, 1995 *Cosmic Winds and the Heliosphere* ed J R Jokipii *et al* (Tucson, AZ: University of Arizona Press)
[36] Berezinskii V S *et al*, 1990 *Astrophysics of Cosmic Rays* (Amsterdam: North-Holland)
[37] Hagiwara K *et al* (The Particle Data Group), 2002 *Phys. Rev.* D **66** 010001 [SPIRES]

JCAP 09(2003)005